

Article

Estimation Error Based Disturbance Observer Design for Flexible Loop Shaping

Sangmin Suh

Semiconductor Division, Samsung Electronics, Hwaseong-si 18448, Korea; sangmin.suh@samsung.com or sangminsuh@naver.com; Tel.: +82-10-2539-1969

Received: 20 October 2018; Accepted: 18 November 2018; Published: 27 November 2018



Abstract: This note presents an estimation error based disturbance observer (EEDOB) to reduce the effects of external disturbances. In the proposed control structure, a difference between an estimator output and a plant output is considered as an equivalent disturbance. Therefore, when a disturbance appears, the proposed disturbance observer (DOB) is activated. Unlike conventional DOB, this method does not require the plant inverse model or additional stabilizing filters. In addition, the proposed method always satisfies closed loop systems stability, which is definitely different from conventional DOB. To verify the effectiveness, this method was applied to commercial storage systems. From the experimental results, it is confirmed that tracking performance is improved by 23.5%.

Keywords: disturbance rejection; EEDOB; LMI; loop shaping; H_∞ control; stability

1. Introduction

The performance of control systems depends on a plant, a controller and external disturbances and vibrations. To a given plant, the controller should be designed to stabilize the closed loop systems and to meet design specifications, whereas the effect of the external disturbances should be minimized so as not to disturb the closed loop system performance.

For controllers, frequency domain control methods such as proportional–integral–derivative (PID) and lead-lag might be considered. However, the frequency domain design methods cannot be applied to state variable based control such as proximate time optimal control, velocity profile based motion control. However, state space control makes it possible to design such state variable dependent control. In addition, the state space controller can be designed to yield the same functions that frequency domain control affords. Therefore, state space control is more useful and it is important to reduce disturbances with maintaining the state space control structure.

External disturbances are the main factor of performance degradation in the closed loop systems. In order to reduce the effects of the disturbance, traditionally, a disturbance observer (DOB) has been popular. Since 1987 [1], the design scheme has been extensively utilized to reject several kinds of external disturbances.

In permanent magnet linear synchronous motors (PMLSMs), they said that measured disturbances are a combination of lump and periodic when the tasks executed by PMLSM motion systems have periodic and repetitive characteristics. In these systems, base line lumped disturbances are estimated and canceled by DOB [2]. Aerodynamic torque and wind speed are monitored and estimated by DOB in the advanced sliding mode control (SMC) scheme for wind energy conversion systems (WECSs) [3]. The paper said that stability has not been reported in a reaction torque observer (RTOB), which is an application of DOB. In addition, they said the stability is affected by the design parameters of RTOB [4]. For the rejection of external disturbances, a state space disturbance observer was also designed [5]. It was reported that DOB based switching control makes it possible to obtain fast, smooth, and accurate

control performance in the presence of both external disturbances and internal uncertainties. In the methodology, two DOBs were used for reacting different frequency ranges. In addition, for more robustness, Q-filter was optimized [6]. Recently, many types of DOB were well summarized and carefully compared [7].

In addition, a linear matrix inequalities (LMI) based loop shaping method was also applied for disturbance rejection [8]. Even though LMI is generally used for loop shaping methods [9–11], it cannot afford relative stability. To remedy the limitation, regional pole placements via LMIs satisfying α -stability were developed [12] and these results were extended to general pole assignment regions and to structured uncertainty [13].

One of the main applications of DOB is hard disk drives [14,15]. In these papers, the structures of hard disk drives and their key components are presented. Regarding the servo controllers, it was said that the state space design is preferable because the same control structure should be used for both seek and track following control. Seek control is point-to-point control and its design goal is to minimize track-to-track movement without exciting structural vibrations. Therefore, time optimal control and velocity profile based control are generally used and the read/write time is highly dependent on this seek time. Thus, seek control is definitely based on state estimator based state space control. Meanwhile, the track following control is regulation control; this tells us how precisely the read/write heads reside on a track. As track following control, frequency domain controllers (such as PID, lead-lag) were used. However, today state estimator based state space pole placement control is popular because state variables are very informative. Including the control problems, the state variable itself tells valuable information of control systems to the host CPU, thus, makes it possible to answer emergency situations. The track following performance is defined by track-misregistration (TMR) based position error signal (PES), which determines tracks-per-inch (TPI). TPI is a critical factor to determine the data capacity of hard disk drives. In hard disk drives, state space DOB has been developed [5] and the proposed DOB does not destroy stability by designing a stable FIR filter. As another method, intentionally designed stable parallel structure was also proposed [8,16].

Conventional DOB consists of two functions, a disturbance monitoring and extracting filter and a stabilizing filter. As the disturbance monitoring and extracting filter, inverse plant model, P_n^{-1} is used, the stabilizing Q-filter is used for closed loop systems stability. Since P_n^{-1} should be designed with considering internal stability and causality, mirroring filters by using all pass filters and low pass filters with far poles should be additionally designed. In addition, the stabilizing filter should be iteratively designed by verifying the stability of closed loop systems. However, the designed DOB cannot tell how to affect frequency responses of the overall closed loop systems because DOB can locally monitor and only remove the disturbances. Thus, even if DOB is effective on disturbance rejection, the design of P_n^{-1} and Q filters are inevitable and they are time-consuming iterative jobs.

This note proposes an estimation error based disturbance observer. The main idea is to remove P_n^{-1} and Q and to provide design flexibility of the closed loop systems without destroying stability. In the steady state, the difference between an estimator output and a plant output (i.e., estimation error) is zero. However, if disturbances are introduced, the error would fluctuate. Therefore, in this note, the difference between an estimator output and a plant output is considered as the equivalent disturbances. Of course, model uncertainty could make the differences but the disturbances caused by model uncertainty are located at high frequency range and such effects are negligible because the plant cannot be activated to such high frequency disturbances. The problem arises only when disturbances located in interesting frequency range come into our systems. Note that when disturbances are introduced the difference appears. This means that this signal can be used as an input of the proposed DOB. In addition, no additional disturbance monitoring and extracting functions are not required because when the disturbance disappears the difference also disappears. Then, a stabilizing controller corresponding to a Q-filter should be designed. The controller should always stabilize the closed loop systems and it can be designed to take a form of the desired frequency response of the closed loop

systems. For that one, this note suggests a new design frame work based on convex optimization, which always satisfies the stability of the closed loop systems.

This note has following contributions. Unlike conventional DOB,

- The proposed method does not require the plant's inverse model.
- It does not need an iterative design process, such as Q -filter design, thus, the proposed method is a systematic design method.
- This method yields design flexibility of the closed loop systems in the state space. Therefore engineers can design arbitrary forms of the closed loop systems.
- In addition, periodic disturbances can be removed by simply adding weighting functions including lumped disturbances.
- The suggested method always guarantees the closed loop systems stability.

This note is organized as follows. Section 2 illustrates a plant modeling and a current estimator based state feedback controller. In Section 3, conventional DOB and its limitations are presented. Section 4 contains a design method of estimation error based disturbance observer (EEDOB) to reduce the influence of external disturbances. In Section 5, experimental results verify the effectiveness of the proposed design method and the conclusion follows. Throughout the note, hard disk drives systems are considered.

2. Plant Modeling and State Feedback Controller Design

From the measurement data, the full model $G_p(s)$ is identified, and for control design, a simplified 2nd order plant model with one low frequency pole $G_n(s)$ is used as follows.

$$\begin{aligned} G_p(s) &= G_n(s) \cdot G_{res}(s) \cdot G_{high}(s) \\ &= \left(\frac{K_t}{J_m} \cdot \frac{1}{s^2 + (B_d/J_m)s + K_s/J_m} \right) \cdot \left(\frac{\omega_n^2}{s^2 + 2\zeta_n\omega_n s + \omega_n^2} \right) \cdot \left(\prod_{i=1}^M \frac{s^2 + 2\zeta_{zi}\omega_{zi}s + \omega_{zi}^2}{s^2 + 2\zeta_{pi}\omega_{pi}s + \omega_{pi}^2} \cdot \frac{\omega_{pi}^2}{\omega_{zi}^2} \right) \end{aligned} \quad (1)$$

where $G_n(s)$, $G_{res}(s)$ and $G_{high}(s)$ are nominal model, high frequency resonance model, and detailed high frequency dynamics of the plant respectively. K_t , J_m , B_d and K_s are the torque constant, inertia, damping coefficient and spring coefficient, which determine low frequency poles. ω_n and ζ_n describe a base line of high frequency characteristics, and the remaining terms represent detailed high frequency features over the base line. For the high frequency dynamics modeling, we choose $M = 2$.

Figure 1 shows the measurement, identified model for analysis, and nominal model for controller design, respectively. The discretized model of $G_n(s)$ is given by

$$P := \begin{cases} x_p(k+1) = A_p x_p(k) + B_p u_p(k) \\ y_p(k) = C_p x_p(k) \end{cases} \quad (2)$$

The current estimator based state feedback controller was designed so that closed loop systems can be stable.

$$C := \begin{cases} \hat{x}_e(k+1) = x_e(k) + L(y_p(k) - C_e x_e(k)) \\ x_e(k+1) = A_e \hat{x}_e(k) + B_e u_{sf}(k) \\ u_{sf}(k) = -K \hat{x}_e(k) \end{cases} \quad (3)$$

where L is a gain of the current estimator, and K is a state-feedback control gain of C . To design Equation (3), we used a pole placement method [17,18]. With the design method, the designed open loop transfer function is shown in Figure 2.

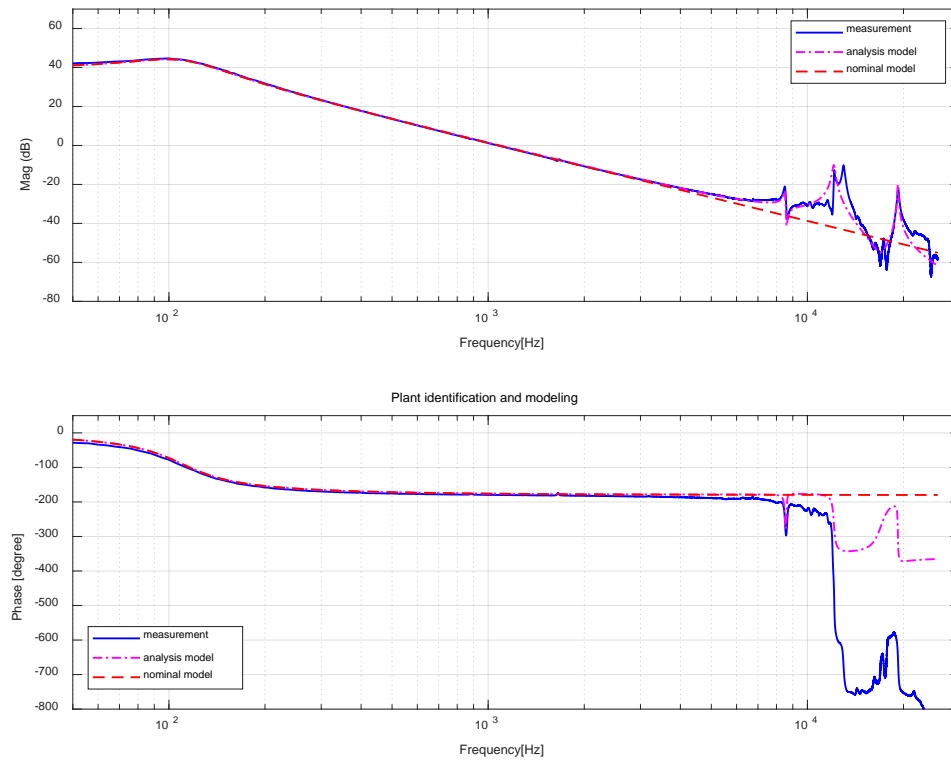


Figure 1. Plant dynamics: Measurement, model for analysis and nominal model for design.

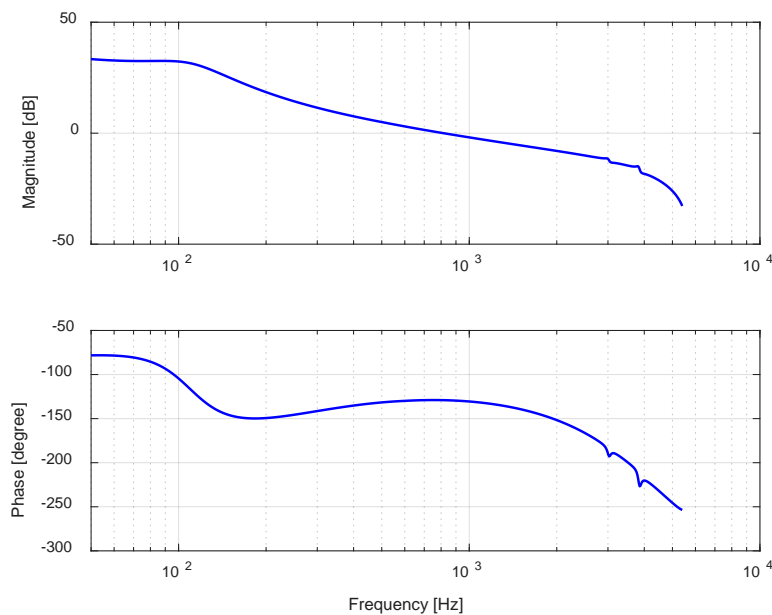


Figure 2. Open loop transfer function.

As 0 dB crossover frequency, 900 Hz was selected to obtain reasonable stability margins. Lag characteristics were observed at a low frequency range whereas lead characteristics were shown at the middle frequency range. The lead feature affords stability to the closed loop systems. Therefore, C stabilizes the closed loop systems without external disturbances.

3. Conventional Disturbance Observer (DOB)

In the presence of external disturbance, DOB has been popular as shown in Figure 3 [1].

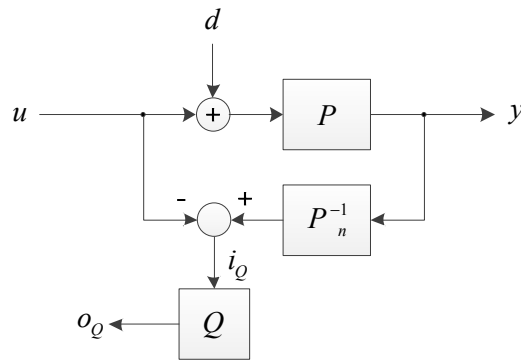


Figure 3. Conventional disturbance observer (DOB).

In the figure, P_n is a nominal model and the input of Q is $i_Q = -u + P_n^{-1}P(d + u)$. Thus, if the real model P and nominal model P_n are identical, then $i_Q = d$. Therefore, the estimated i_Q goes to filter Q and the filtered o_Q is subtracted from u . Since P_n is generally strictly proper, additional filters are required to increase the degree of the denominator for calculating P_n^{-1} . Moreover, if P_n is a non-minimum plant, a mirroring filter by using all pass filter is also designed. As the Q filter determines the stability of DOB by controlling the bandwidth of the disturbances, the Q filter should be iteratively designed with verifying stability. In this note, the author would like to remove those processes without destroying stability.

To evaluate the design flexibility of a usual DOB [7], frequency responses of the closed loop systems with various Q filters should be investigated. In this example, P_n^{-1} is non-proper and as a Q filter $\omega_Q^2 / (s^2 + 2 \cdot 0.707 \cdot \omega_Q s + \omega_Q^2)$ was selected for its steep slope in the high frequency range. In addition, the filter bandwidth ω_Q without destroying stability was searched by trial and error. Finally, closed loop systems with various bandwidth Q filters were obtained.

As the filter bandwidth ω_Q increases, the bandwidths of the open loop functions also increase and therefore the peaks of plant input sensitivity functions (y/d) decrease. Figure 4 shows the trend. This means a conventional DOB effectively reduces the effects of the introduced disturbances. However, the designed closed loop functions are located in the bounded area. Moreover, the disturbance attenuation rates are similar in all of the frequency ranges. Therefore, a conventional DOB has limitations to selectively reduce disturbances or design flexible loop shaping in the closed loop systems.

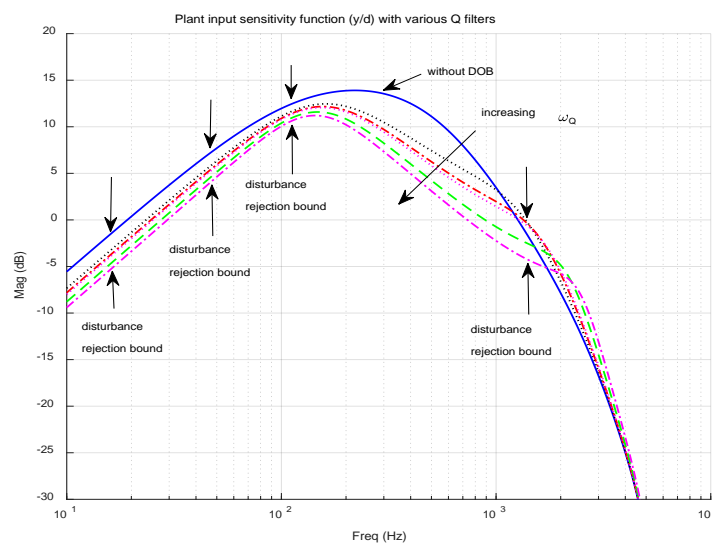


Figure 4. Feature of conventional DOB.

4. Estimation Error Based DOB Design

This section contains the main results of this note. First, we briefly present a control structure and its features and suggest a systematic design method of weighting functions to help find feasible solutions in LMIs optimization. Then, an augmented plant to find an LMI based EEDOB was formulated. Finally, the EEDOB (E) was designed by using the suggested weighting function.

4.1. Proposed Control Structure

The proposed control structure is illustrated in Figure 5 and has the following properties.

- No plant inverse model or stabilizing Q filter is required.
- The input of EEDOB is the difference between the estimator output and plant output, $y_p(k) - \hat{y}_e(k)$.
- If external disturbances are introduced into P in a steady state, $|y_p(k) - \hat{y}_e(k)|$ increases.
- EEDOB can help reject the error to reduce the effects of disturbances by injecting a counter acting control effort.
- If the disturbance disappears, the estimation error converges to zero and finally, the EEDOB is not activated any more.

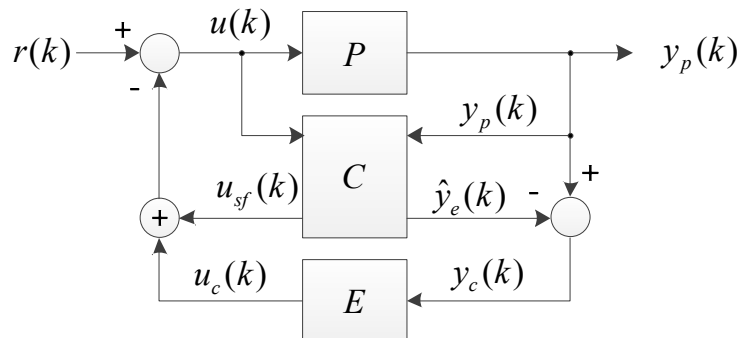


Figure 5. Proposed control structure.

In Figure 5, $\hat{y}_e(k) = C_e \hat{x}_e(k)$ is an estimation output based on a current state variable. $y_c(k)$ and $u_c(k)$ are the input and output of the proposed DOB. Since the proposed controller is activated only when external disturbances are introduced, we can utilize this controller as a disturbance observer.

4.2. Weighting Function Design

To reduce the influence of external disturbances, a peak of plant input sensitivity function should be reduced and the weighting function for the control design must be able to express the desired frequency response.

Let S_i be a plant input sensitivity function defined by a transfer function from $u(k)$ to $y_p(k)$ without EEDOB, and we suggest F_{pk} describes a peak of S_i as follows [16].

$$F_{pk} = D \left(\mu \frac{s + \omega_{c1}}{s + \mu \omega_{c1}} \cdot \frac{s/\mu + \omega_{c2}}{s + \omega_{c2}} \right) \quad (4)$$

where $D(\cdot)$ is a discretization operator denoting bilinear transformation, s is a complex variable in laplace transform, ω_{c1} and ω_{c2} are two cutoff frequencies of S_i , $\mu = 10^{(m_p/20)}$, and m_p is the peak of S_i . Then, a desired plant input sensitivity function can be represented by

$$W^{-1} = S_i \cdot F_{pk}^{-1}. \quad (5)$$

Since S_i is multiplied by F_{pk}^{-1} , a peak of W^{-1} should be lower than that of S_i . Accordingly, if we use W as a weighting function, an improved plant input sensitivity function with a lower peak can be obtained. In addition, if repetitive sharp disturbances are introduced, such periodic disturbances can be also cancelled by simply modifying W^{-1} as follows

$$\begin{aligned} W^{-1} &= W^{-1} \cdot \prod_{n=1}^L N_n^{-1} \\ &= S_i \cdot F_{pk}^{-1} \cdot \prod_{n=1}^L N_n^{-1} \end{aligned} \quad (6)$$

where, $N_n^{-1} = D\left(\frac{s^2 + 2\zeta_n\omega_n s + \omega_n^2}{s^2 + 2\zeta_n\omega_n s + \omega_n^2}\right)$

where N_n^{-1} is a notch filter to reduce the periodic disturbances located at ω_n . The depth and width of the notch filter are controlled by ζ_n . In this note, the periodic disturbance is not considered for simplicity. In addition, if we face two problems to design W , which are causality and stability. Those problems can be successfully resolved by using zero gain error tracking control (ZGETC) [16] and zero phase error tracking control (ZPETC) [19]. In order to show clear design concepts, S_i , F_{pk}^{-1} , and W^{-1} are illustrated in Figure 6.

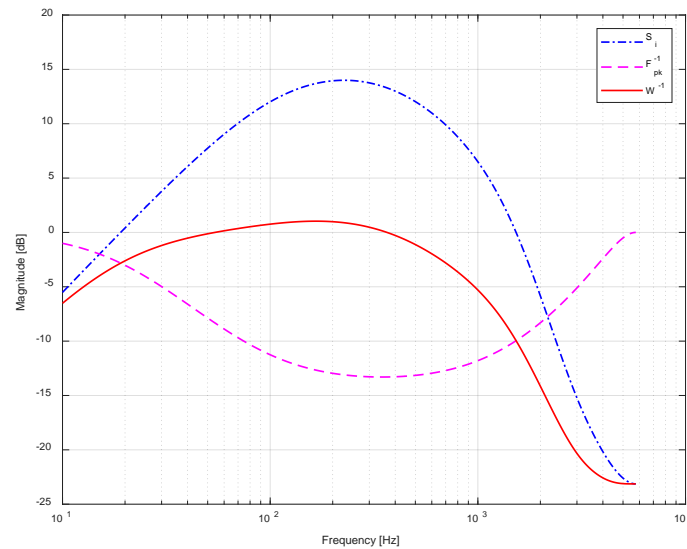


Figure 6. Frequency responses of S_i , F_{pk}^{-1} , and W^{-1} .

4.3. EEDOB Design Based on LMI Optimization

A block diagram of augmented and generalized systems for EEDOB design is shown in Figure 7. Using the block diagram, an LMI framework was designed to obtain an H_∞ controller.

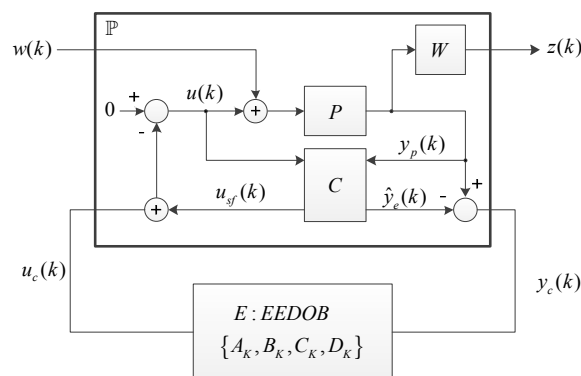


Figure 7. Design frame work of the proposed EEDOB.

Using Equations (2) and (3), the plant state equation can be represented by

$$\begin{aligned}
 x_p(k) &= A_p x_p(k) + B_p (w(k) + u_p(k)) \\
 &= A_p x_p(k) + B_p (w(k) - u_{sf}(k) - u_c(k)) \\
 &= A_p x_p(k) + B_p (w(k) - K \hat{x}_e(k) - u_c(k)) \\
 &= A_p x_p(k) + B_p (w(k) - K((I - LC_e)x_e(k) + LC_p x_p(k)) - u_c(k)) \\
 &= A_p x_p(k) - B_p K(I - LC_e)x_e(k) - B_p KLC_p x_p(k) + B_p w(k) - B_p u_c(k) \\
 &= (A_p - B_p KLC_p)x_p(k) - B_p K(I - LC_e)x_e(k) + B_p w(k) - B_p u_c(k).
 \end{aligned} \tag{7}$$

In addition, the estimator state equation is also written by

$$\begin{aligned}
 x_e(k) &= A_e \hat{x}_e(k) + B_e u_p(k) \\
 &= A_e \hat{x}_e(k) + B_e (-K \hat{x}_e(k) - u_c(k)) \\
 &= (A_e - B_e K) \hat{x}_e(k) - B_e u_c(k) \\
 &= (A_e - B_e K)(I - LC_e)x_e(k) + (A_e - B_e K)LC_p x_p(k) - B_e u_c(k) \\
 &= (A_e - B_e K)LC_p x_p(k) + (A_e - B_e K)(I - LC_e)x_e(k) - B_e u_c(k).
 \end{aligned} \tag{8}$$

W in Equation (5) is reformulated by a state-space representation as shown in Equation (9).

$$W := \begin{cases} x_w(k+1) = A_w x_w(k) + B_w u_w(k) \\ y_w(k) = C_w x_w(k) + D_w u_w(k) \end{cases}. \tag{9}$$

Then, the state equation of W can be written by

$$\begin{aligned}
 x_w(k+1) &= A_w x_w(k) + B_w y_p(k) \\
 &= B_w C_p x_p(k) + A_w x_w(k).
 \end{aligned} \tag{10}$$

The signal to be minimized is

$$\begin{aligned}
 z(k) &= C_w x_w(k) + D_w y_p(k) \\
 &= D_w C_p x_p(k) + C_w x_w(k).
 \end{aligned} \tag{11}$$

In addition, the measurement signal, $y_c(k)$, is

$$\begin{aligned}
 y_c(k) &= y_p(k) - \hat{y}_e(k) \\
 &= C_p x_p(k) - C_e \hat{x}_e(k) \\
 &= C_p x_p(k) - C_e ((I - LC_e)x_e(k) + LC_p x_p(k)) \\
 &= C_p x_p(k) - C_e ((I - LC_e)x_e(k) + LC_p x_p(k)) \\
 &= (C_p - C_e LC_p)x_p(k) - C_e (I - LC_e)x_e(k).
 \end{aligned} \tag{12}$$

Therefore, from Equations (7) (8) (10) (11) and (12), the generalized plant can be written by

$$\begin{aligned}
 x(k+1) &= Ax(k) + B_1 w(k) + B_2 u_c(k) \\
 z(k) &= C_1 x(k) + D_{11} w(k) + D_{12} u_c(k) \\
 y_c(k) &= C_2 x(k) + D_{21} w(k) + D_{22} u_c(k)
 \end{aligned} \tag{13}$$

where $x(k) = \begin{bmatrix} x_p^T(k) & \bar{x}_e^T(k) & \bar{x}_w^T(k) \end{bmatrix}$, and

$$\begin{aligned}
 A &= \begin{bmatrix} A_p - B_p KLC_p & -B_p K(I - LC_e) & 0 \\ (A_e - B_e K)LC_p & (A_e - B_e K)(I - LC_e) & 0 \\ B_w C_p & 0 & A_w \end{bmatrix}, \quad B_1 = \begin{bmatrix} B_p \\ 0 \\ 0 \end{bmatrix}, \quad B_2 = \begin{bmatrix} -B_p \\ -B_e \\ 0 \end{bmatrix}, \\
 C_1 &= \begin{bmatrix} D_w C_p & 0 & C_w \end{bmatrix}, \quad D_{11} = 0, \quad D_{12} = 0, \\
 C_2 &= \begin{bmatrix} C_p - C_e LC_p & -C_e (I - LC_e) & 0 \end{bmatrix}, \quad D_{21} = 0, \quad D_{22} = 0.
 \end{aligned} \tag{14}$$

In addition, a state space representation of EEDOB is defined by

$$E(\text{EEDOB}) := \begin{cases} \Sigma(k+1) = A_K \Sigma(k) + B_K y_c(k) \\ u_c(k) = C_K \Sigma(k) + D_K y_c(k) \end{cases} \quad (15)$$

Then, the closed loop systems, T_{zw} , can be written by

$$\begin{bmatrix} x(k+1) \\ \Sigma(k+1) \end{bmatrix} = \begin{bmatrix} A + B_2 D_K C_2 & B_2 C_K \\ B_K C_2 & A_K \end{bmatrix} \begin{bmatrix} x(k) \\ \Sigma(k) \end{bmatrix} + \begin{bmatrix} B_1 + B_2 D_K D_2 \\ B_K D_{21} \end{bmatrix} w(k) \quad (16)$$

$$z(k) = \begin{bmatrix} C_1 + D_{12} D_K C_2 & D_{12} C_K \end{bmatrix} \begin{bmatrix} x(k) \\ \Sigma(k) \end{bmatrix} + (D_{11} + D_{12} D_K D_{21}) w(k).$$

Theorem 1. The following two statements in Equations (17) and (18) are equivalent.

$$\|T_{zw}\|_\infty^2 = \sup_{w \neq 0} \frac{\|z\|_2^2}{\|w\|_2^2} < \gamma \quad (17)$$

$$\begin{bmatrix} X & I & AX + B_2 L & A + B_2 R C_2 & B_1 + B_2 R D_{21} & 0 \\ * & Y & Q & YA + F C_2 & Y B_1 + F D_{21} & 0 \\ * & * & X & I & 0 & X^T C_1^T + L^T D_{12}^T \\ * & * & * & Y & 0 & C_1^T + C_2^T R^T D_{12}^T \\ * & * & * & * & I & D_{11}^T + D_{21}^T R^T D_{12}^T \\ * & * & * & * & * & \gamma I \end{bmatrix} > 0 \quad (18)$$

where Q, F, L, R and symmetric matrices X, Y are variables. $X > 0$ means that X is positive definite, and $*$ denotes an ellipsis for terms induced by a symmetric matrix, i.e.,

$$\begin{bmatrix} A & B \\ B^T & C \end{bmatrix} = \begin{bmatrix} A & B \\ * & C \end{bmatrix}. \quad (19)$$

Proof. The result immediately follows from [11,20–22].

Therefore, $\|T_{zw}\|_\infty$ can be minimized by minimizing γ subject to Equation (18). The feasible controller is given by choosing nonsingular V and U such that $Y_{opt} X_{opt} + VU = I$ and calculating

$$\begin{aligned} D_K &= R_{opt}, \\ C_K &= (L_{opt} - R_{opt} C_2 X_{opt}) U^{-1}, \\ B_K &= V^{-1} (F_{opt} - Y_{opt} B_2 R_{opt}), \\ A_K &= V^{-1} (Q_{opt} - Y_{opt} (A + B_2 R_{opt} C_2) X_{opt} - V B_K C_2 X_{opt}) U^{-1} - V^{-1} Y_{opt} B_2 C_K \end{aligned} \quad (20)$$

where the subscript $(\cdot)_{opt}$ denotes an optimal solution of a corresponding variable.

Theorem 2. The closed loop systems as shown in Figure 7 are stable.

Proof. Since the controller EEDOB given by H_∞ dynamic out feedback control always stabilizes an augmented plant \mathbb{P} [9–11], the closed loop system is stable.

The proposed method can afford complete design flexibility and indeed remove external disturbances taking arbitrary forms in the frequency domain. However, as a disturbance spectrum to be removed becomes complicated, the weighting function W becomes complicated as well. This means that with high order weighting, a high order controller is designed. Let $O(\cdot)$ be an

order, then, $O(E) = O(P) + O(C) + O(W)$. Another thing to be considered is the computational time. Computations should be done within a sampling time. However, if a calculation time is longer than the sampling time, the desired performance cannot be achievable or the closed loop systems cannot be controllable. Accordingly, the critical disturbance affecting to closed loop system performance should be first removed. All disturbances cannot be removed in the control systems. As a result, this method can precisely shape a frequency response of the closed loop systems and grants complete design flexibility at the cost of computational efforts.

5. Experimental Results

The proposed design method was applied to a hard disk drive with 3600 rpm and 86.8 μ s sample rate. All data were obtained from 600 times experiments.

In order to measure the sensitivity functions as shown in Figure 8, sin wave $i_{\sin}(k)$ was repetitively (600 times) introduced to the position signal and $o_{\sin}(k)$ was measured. The measured values were averaged to reduce measurement noises.

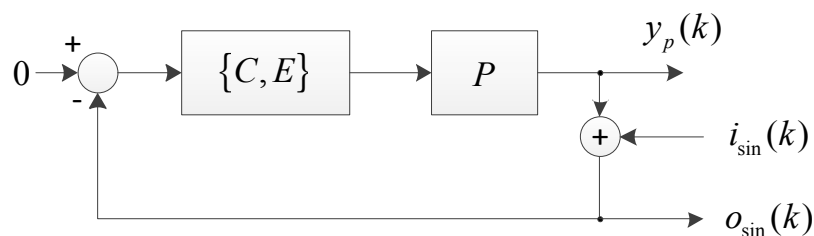


Figure 8. Measurement method of frequency responses.

Frequency responses of the plant input sensitivity functions are compared in Figure 9.

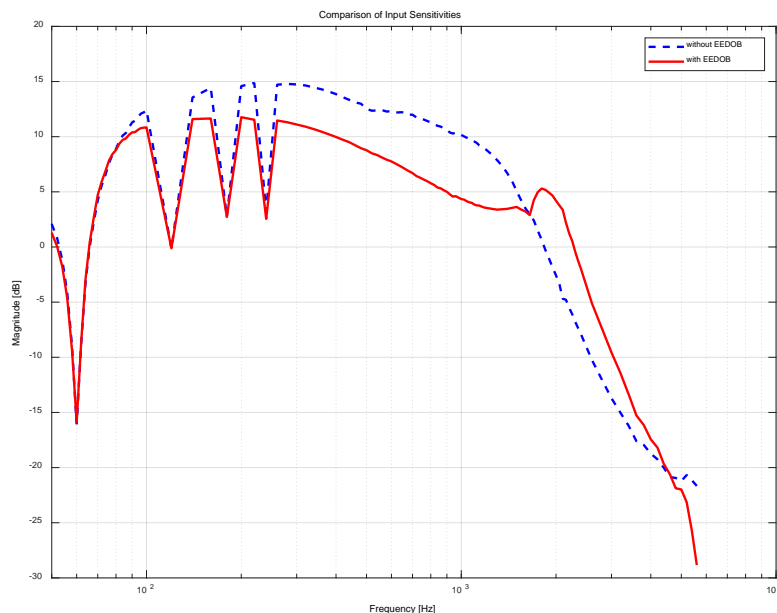


Figure 9. Input sensitivity functions from plant input disturbance to plant output.

In the input sensitivity function, at an area above 0 dB, the introduced disturbances were not decreased but amplified. Thus, at least, the area should be reduced. The maximum peak of the input sensitivity function decreased from 15 dB to 11.5 dB. With EEDOB, the width of the amplification area increased and this means that the proposed EEDOB deteriorates the disturbance rejection performance in that area. However, the total area located at above 0 dB was reduced and this result was verified by the final power spectral density. In hard disk drives servo systems, iterative learning controllers were

implemented to reduce periodic disturbances. In this note, four controllers were activated. However, instead of the iterative learning controllers, such period disturbances can be also reduced by simply adding $\prod_{n=1}^M N_n^{-1}$ in (6). M is the number of the period disturbances to be canceled.

Figure 10 shows the compared frequency responses of plant output sensitivity functions. Since the proposed EEDOB increased the bandwidth from 622.8 Hz to 944.7 Hz, the output disturbances located in a frequency ranging from 622.8 Hz to 944.7 Hz were additionally reduced by the proposed EEDOB. With increasing the bandwidth by 320 Hz, the peak increased by 1.05 dB according to the Bode integral theorem [21].

Frequency responses of the open loop transfer functions are written in Figure 11. With EEDOB, a crossover frequency increased from 923.4 Hz to 1420 Hz. With EEDOB, the phase margin was almost preserved from 27.13° to 27.8° , whereas the gain margin was slightly reduced by 1 dB.

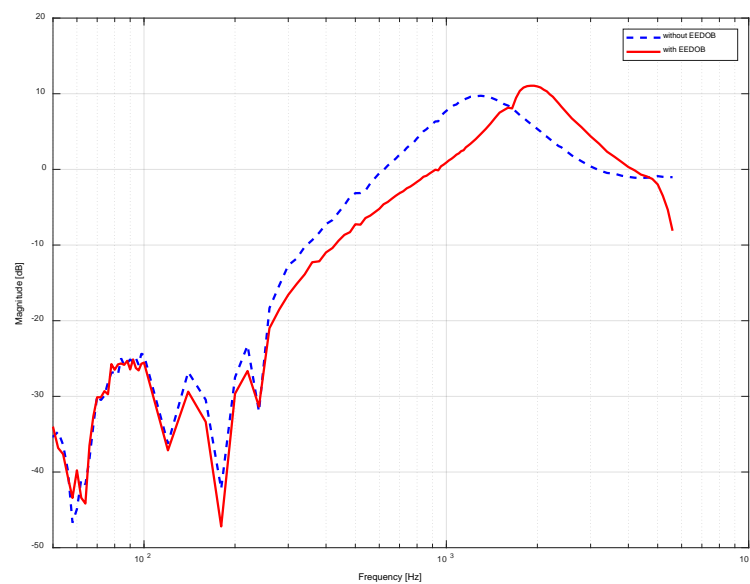


Figure 10. Output sensitivity functions from plant output disturbance to plant output.

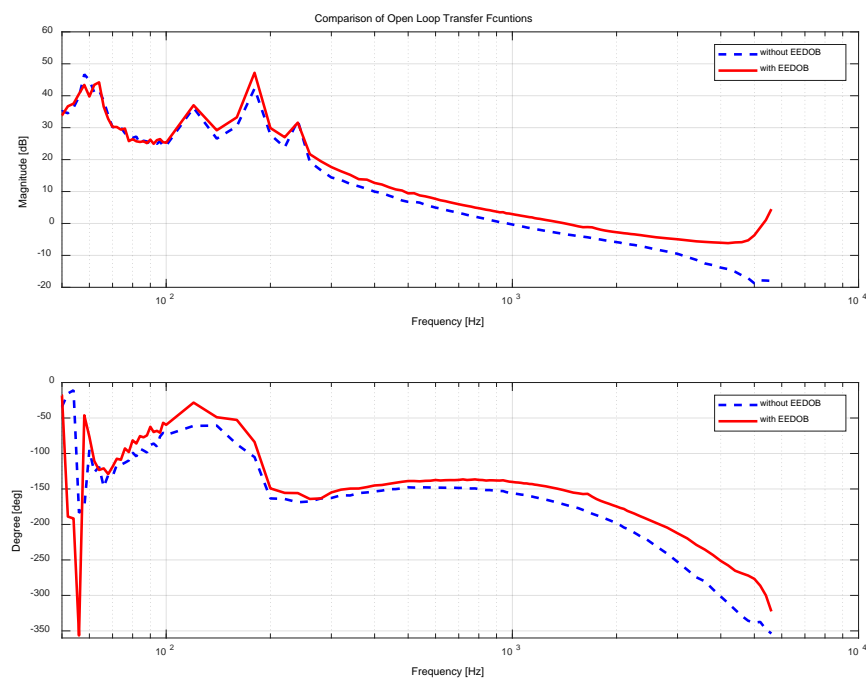


Figure 11. Measured open loop transfer functions.

For tracking performances comparison, power spectral densities (PSD) are illustrated in Figure 12. A cumulated sum of the PSD decreased from 0.89% to 0.68%. Therefore, tracking performance is enhanced by around 23.5% and this means the data capacity can be increased by the proposed method.

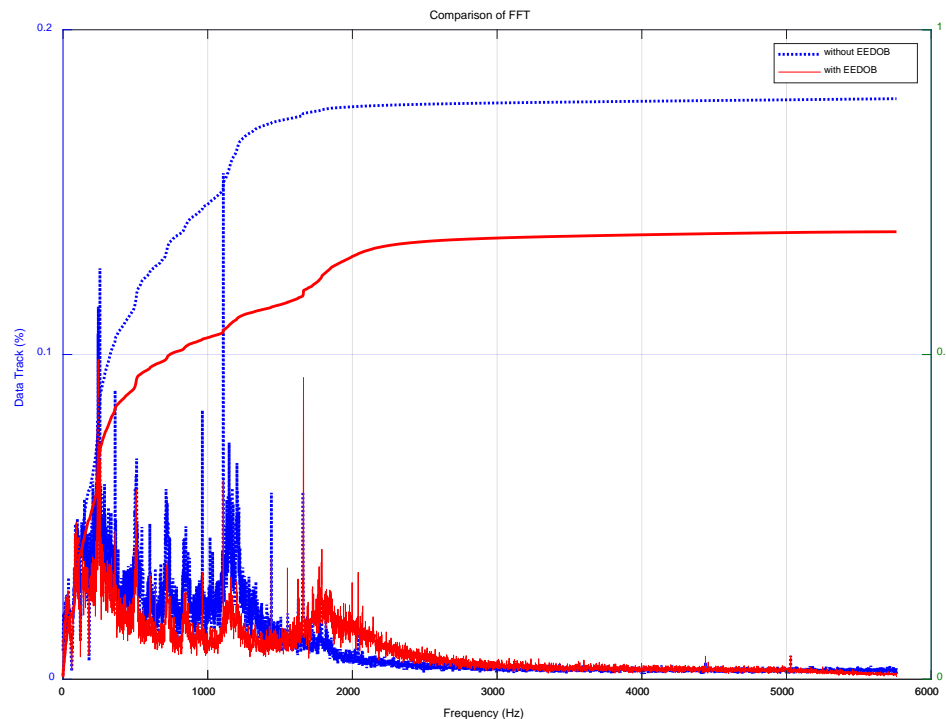


Figure 12. Power spectral density and cumulated sum.

Using data from the experimental results, the frequency characteristics are summarized in Table 1 for readability.

Table 1. Performance of vibration reduction.

Items	Definition	Unit	w/o EEDOB	w/EEDOB
OLTF (f_c)	Cutoff frequency of open loop transfer function	Hz	923.4	1420
OLTF (GM)	Gain margin of the open loop transfer function	dB	4.16	3.15
OLTF (PM)	Phase margin of the open loop transfer function	degree ($^\circ$)	27.13	27.8
PISF (peak)	Maximum peak of plant input sensitivity function from plant input disturbance to plant output	dB	15	11.5
POSF (peak)	Maximum peak of plant output sensitivity function from plant output disturbance to plant output	dB	10	11.05
POSF (BW)	Bandwidth of plant output sensitivity function from plant output disturbance to plant output	Hz	622.8	944.7
PSD	Power spectral density of PES	Percentage of 3σ	0.89	0.68

6. Conclusions

This note proposes an estimation error based disturbance observer to reject external disturbances. A difference between an estimator output and a plant output is considered as an equivalent disturbance. Therefore, when a disturbance appears, the proposed disturbance observer (DOB) is activated. The proposed method requires no inversion model or iterative calculations of the Q -filter design and the designed closed loop systems are always stable. The experimental results with commercial hard disk drives confirm the validity and effectiveness of the proposed method. With the suggested method, tracking performance was improved by 23.5%.

This note has contributions as follows. Unlike conventional DOB,

- It needs no plant inverse model or iteratively designed stabilizing Q filter. Therefore, this method is a systematically designed one.
- It yields design flexibility of the closed loop systems.
- It can reduce repetitive disturbances by simply adding corresponding weights.
- It always guarantees closed loop system stability because the proposed framework is on the basis of H_∞ dynamic out feedback.

Funding: This research received no external funding.

Acknowledgments: The author would like to appreciate the anonymous reviewers for their valuable comments and suggestions that have contributed to improve this manuscript.

Conflicts of Interest: The author declares no conflicts of interest.

References

1. Ohnishi, K. A New Servo Method in Mechatronics. *Trans. Jpn. Soc. Electr. Eng.* **1987**, *107-D*, 83–86.
2. Cho, K.; Kim, J.; Choi, S.B.; Oh, S. A High-Precision Motion Control Based on a Periodic Adaptive Disturbance Observer in a PMLSM. *IEEE/ASME Trans. Mechatron.* **2015**, *20*, 2158–2171. [[CrossRef](#)]
3. Do, T.D. Disturbance Observer-Based Fuzzy SMC of WECSs without Wind Speed Measurement. *IEEE Access* **2017**, *5*, 147–155. [[CrossRef](#)]
4. Sariyildiz, E.; Ohnishi, K. Stability and Robustness of Disturbance-Observer-Based Motion Control Systems. *IEEE Trans. Ind. Electr.* **2015**, *62*, 414–422. [[CrossRef](#)]
5. Suh, S.; Chung, C.C.; Lee, S.-H. Discrete-Time Track Following Controller Design Using a State-Space Disturbance Observer. *Microsyst. Technol.* **2003**, *9*, 352–361. [[CrossRef](#)]
6. Wang, L.; Su, J.; Xiang, G. Robust Motion Control System Design With Scheduled Disturbance Observer. *IEEE Trans. Ind. Electr.* **2016**, *63*, 6519–6529. [[CrossRef](#)]
7. Chen, W.H.; Yang, J.; Guo, L.; Li, S. Disturbance-observer-based control and related methods—An overview. *IEEE Trans. Ind. Electr.* **2016**, *63*, 1083–1095. [[CrossRef](#)]
8. Suh, S. Unified H_∞ Control to Suppress Vertices of Plant Input and Output Sensitivity. *IEEE Control Syst. Technol.* **2010**, *18*, 969–975. [[CrossRef](#)]
9. Boyd, S.; Ghaoui, L.E.; Feron, E.; Balakrishnan, V. *Linear Matrix Inequalities in System and Control Theory*; SIAM: Philadelphia, PA, USA, 1994.
10. Gahinet, P.; Nemirovskii, A.; Laub, A.J.; Chilali, M. The LMI control toolbox. In Proceedings of the 1994 33rd IEEE Conference on Decision and Control, Lake Buena Vista, FL, USA, 14–16 December 1994.
11. Oliveira, C.D.; Geromel, J.C.; Bernussou, J. An LMI optimization approach to multiobjective controller design for discrete-time systems. In Proceedings of the 38th Conference on Decision and Control, Phoenix, AZ, USA, 7–10 December 1999; Volume 4, pp. 3611–3616.
12. Chilali, M.; Gahinet, P. H_∞ design with α -stability constraint: An LMI approach. In Proceedings of the 1994 33rd IEEE Conference on Decision and Control, Lake Buena Vista, FL, USA, 14–16 December 1994; pp. 307–312.
13. Chilali, M.; Gahinet, P. H_∞ design with pole placement constraints: An LMI approach. *IEEE Trans. Autom. Cont.* **1996**, *41*, 358–367. [[CrossRef](#)]
14. Abramovitch, D.; Franklin, G.F. A brief history of disk drive control. *IEEE Control Syst.* **2002**, *22*, 28–42. [[CrossRef](#)]
15. Messner, W.; Ehrlich, R. A tutorial on controls for disk drives. In Proceedings of the 2001 American Control Conference (Cat. No.01CH37148), Arlington, VA, USA, 25–27 June 2001; pp. 408–420.
16. Suh, S. Discrete-time controller design to attenuate effects of external disturbances. *Microsyst. Technol.* **2009**, *15*, 1645. [[CrossRef](#)]
17. Åström, K.J.; Wittenmark, B. *Computer-Controlled Systems Theory and Design*, 3rd ed.; Prentice Hall: Englewood Cliffs, NJ, USA, 1997.
18. Franklin, G.F.; Powell, J.D.; Workman, M.L. *Digital Control of Dynamic Systems*; Addison-Wesley: Boston, MA, USA, 1990.

19. Tomizuka, M. Zero phase error tracking algorithm for digital control. *ASME J. Dyn. Syst. Meas. Control* **1987**, *109*, 65–68. [[CrossRef](#)]
20. Burl, J.B. *Linear Optimal Control*; Addison-Wesley: Boston, MA, USA, 1999.
21. Skogestad, S.; Postlethwaite, I. *Multivariable Feedback Control: Analysis and Design*; Wiley: New York, NY, USA, 1996.
22. Zhou, K.; Doyle, J.C.; Glover, K. *Robust and Optimal Control*; Prentice Hall: Englewood Cliffs, NJ, USA, 1996.



© 2018 by the author. Licensee MDPI, Basel, Switzerland. This article is an open access article distributed under the terms and conditions of the Creative Commons Attribution (CC BY) license (<http://creativecommons.org/licenses/by/4.0/>).